DAMAGE GROWTH AFFECTED BY FRICTIONAL SLIP AND DILATANCY AT CRACK INTERFACES

A. Seweryn[1], R. D. Kulchytsky-Zhyhailo[1] and Z. Mróz[2]
[1] Faculty of Mechanical Engineering, Białystok University of Technology, Wiejska 45 C, 15-351 Białystok, Poland,
[2] Polish Academy of Sciences, Institute of Fundamental Technological Research, Świętokrzyska 21, 00-049 Warsaw, Poland

ABSTRACT

A material element with distributed microcracks of arbitrary orientations is considered under tensile and compressive stress regimes. The frictional slip with accompanying dilatancy at rough crack interfaces is assumed and crack growth criterion is derived. The variation of material compliance is analyzed and the non-linear response is determined for proportional loading and unloading.

1. INTRODUCTION

The present paper is aimed at extension of previous studies by considering the contact dilatancy effect. The cracked material element is considered with cracks distributed along specific orientations, (see Figure 1), or arbitrarily distributed. The coupled inelastic phenomena such as crack growth and frictional slip combined with dilatancy affect the material compliance which differs essentially in compressive and tensile stress regimes due to unilateral contact at cracked surfaces. The crack growth within initial plane orientation is assumed and the crack interaction is neglected in the analysis.

2. MODEL FORMULATION

Assume the small strain theory and decompose the strain tensor into elastic and damage components: $\boldsymbol{\varepsilon} = \boldsymbol{\varepsilon}^{\mathrm{e}} + \boldsymbol{\varepsilon}^{\mathrm{d}}$. Assume the Hooke's law for the elastic component $\boldsymbol{\varepsilon}^{\mathrm{e}} = \mathbf{C}\boldsymbol{\sigma}$, where $\mathbf{C}$ denotes the elastic compliance tensor and $\boldsymbol{\sigma}$ is the stress tensor. Consider a representative volume element with m_{V} microcracks. For a continuous distribution of microcracks damage strain tensor can be presented in the form

$$\boldsymbol{\varepsilon}^{\mathrm{d}} = \frac{1}{2\pi}\int_{\Omega}\left[\varepsilon_n^{\mathrm{d}}\mathbf{n}\otimes\mathbf{n} + \mathrm{sym}\left(\boldsymbol{\gamma}_n^{\mathrm{d}}\otimes\mathbf{n}\right)\right]\,\mathrm{d}\Omega\,, \tag{1}$$

where Ω is a semi-plane of the unit radius. The mean damage strain components in the physical plane $\varepsilon_n^{\mathrm{d}}$, $\boldsymbol{\gamma}_n^{\mathrm{d}}$ can be expressed as follows

$$\varepsilon_n^{\mathrm{d}} = c_{\mathrm{n}}\alpha_n^3\left(\sigma_n - p_n\right), \qquad \boldsymbol{\gamma}_n^{\mathrm{d}} = c_{\mathrm{t}}\alpha_n^3\left(\boldsymbol{\tau}_n - \mathbf{f}_n\right), \tag{2}$$

where $\alpha_n = a_n/a_0$ denotes the ratio actual and initial crack size, p_n and $\mathbf{f}_n$ are the contact tractions in normal and tangential directions, c_{n}, c_{t} are the normal and tangential compliance moduli, thus

$$c_{\mathrm{n}} = \frac{m_{\mathrm{V}}a_0^3}{EV}g_{\mathrm{n}}(\nu)\,, \qquad c_{\mathrm{t}} = \frac{m_{\mathrm{V}}a_0^3}{EV}g_{\mathrm{t}}(\nu)\,, \tag{3}$$

and $g_{\mathrm{n}}(\nu)$ and $g_{\mathrm{t}}(\nu)$ are the functions of the Poisson ratio. The stress components acting on a crack plane are expressed by assuming that there is no crack in the physical plane, thus

$$\sigma_n = \mathbf{n}\cdot\boldsymbol{\sigma}\cdot\mathbf{n}\,, \qquad \boldsymbol{\tau}_n = \left(\mathbf{I} - \mathbf{n}\otimes\mathbf{n}\right)\cdot\boldsymbol{\sigma}\cdot\mathbf{n}\,. \tag{4}$$

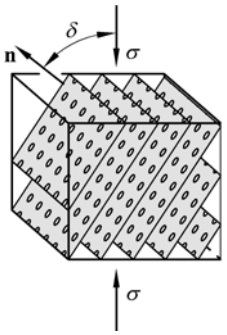

Figure 1: A material element with microcracks: a set of oriented cracks.

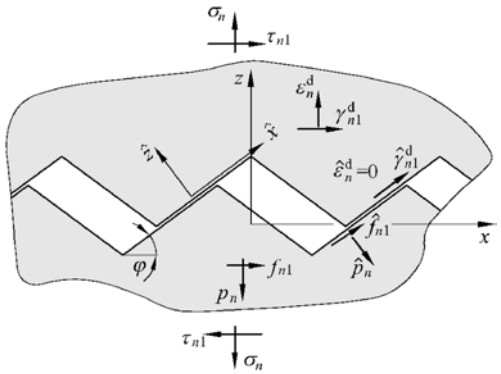

Figure 2: Friction slip and contact forces at inclined crack interface: interaction of wedge asperities.

Assume that the crack growth in a physical plane is not affected by cracks in other planes. For simplicity, consider circular crack growth depending on one parameter, namely the crack diameter a_n. Applying the Griffith energy criterion of crack growth, we state that

$$\Phi_{\mathrm{d}} = G_n - R(\alpha_n) = 0\,, \tag{5}$$

where $R = R(\alpha_n)$ is the crack growth resistance function and G_n denotes the potential energy release due to crack presence:

$$G_n = \frac{3}{2}\alpha_n^2\left[c_{\mathrm{n}}\left(\sigma_n - p_n\right)^2 + c_{\mathrm{t}}\left(\boldsymbol{\tau}_n - \boldsymbol{\gamma}_n\right)\cdot\left(\boldsymbol{\tau}_n - \boldsymbol{\gamma}_n\right)\right]. \tag{6}$$

Thus, we have

$$\begin{aligned} &\mathrm{d}\alpha_n > 0, \quad \text{for} \quad \Phi_{\mathrm{d}} = \mathrm{d}\Phi_{\mathrm{d}} = 0, \\ &\mathrm{d}\alpha_n = 0, \quad \text{for} \quad \Phi_{\mathrm{d}} < 0 \qquad\quad \text{or} \quad \Phi_{\mathrm{d}} = 0, \quad \mathrm{d}\Phi_{\mathrm{d}} < 0. \end{aligned} \tag{7}$$

Consider a circular microcrack in contact on rough surfaces (see Figure 2). Assume the wedge asperities to be inclined at the angle φ to the nominal contact surface Γ_0. The actual rough contact surface is denoted by $\hat{\Gamma}_0$ and the friction coefficient on this surface is denoted by $\mu = \arctan\psi$, where ψ is the friction angle. The quantities referred to the actual inclined interface will be marked by " ^ ", thus $\hat{p}_n$ and $\hat{\mathbf{f}}_n\left(\hat{\mathbf{f}}_{n1}, \hat{\mathbf{f}}_{n2}\right)$, and $\hat{\varepsilon}_n^{\mathrm{d}}$, $\hat{\boldsymbol{\gamma}}_n^{\mathrm{d}}\left(\hat{\boldsymbol{\gamma}}_{n1}^{\mathrm{d}}, \hat{\boldsymbol{\gamma}}_{n2}^{\mathrm{d}}\right)$ denote stress and strain components acting on the asperity surface inclined at the angle φ. The quantities referred to the nominal plane are denoted by p_n, $\mathbf{f}_n$ and $\varepsilon_n^{\mathrm{d}}, \boldsymbol{\gamma}_n^{\mathrm{d}}$. We can distinguish the opening mode O_{m} with no tractions transferred, the slip mode S_{m} with accompanying friction and dilatancy, finally the closure mode C_{m} with no slip (e.g. Mróz and Seweryn [3]).

The opening mode O_{m} occurs when

$$\varepsilon_n^{\mathrm{d}} > \left|\boldsymbol{\gamma}_n^{\mathrm{d}}\right| \tan\varphi \quad \text{and} \quad p_n = 0, \quad \mathbf{f}_n = \mathbf{0}\,. \tag{8}$$

The closure mode C_{m} corresponds to the interaction of a closed crack with no slip. For the Coulomb friction condition, we can write

$$\left|\hat{\mathbf{f}}_n\right| < -\hat{p}_n \tan\psi \quad \text{and} \quad p_n = \sigma_n, \qquad \mathbf{f}_n = \boldsymbol{\tau}_n, \quad \varepsilon_n^{\mathrm{d}} = 0, \quad \boldsymbol{\gamma}_n^{\mathrm{d}} = 0, \quad G_n = 0\,. \tag{9}$$

The closed microcracks with no slip do not affect the material compliance or stress distribution.

The contact slip mode C_{m} occurs when

$$\left|\boldsymbol{\tau}_n\right| \geq \frac{c_{\mathrm{n}}}{c_{\mathrm{t}}}\sigma_n \cot\varphi \tag{10}$$

and the limit friction condition must be satisfied on the inclined contact surface, thus

$$\left|\hat{\mathbf{f}}_n\right| = -\hat{p}_n \tan\psi\,. \tag{11}$$

When the inequality (8) is satisfied, the deformation process occurs with open crack mode. The crack growth condition (5) now takes the form

$$\Phi_{\mathrm{d}} = \frac{3}{2}\alpha_n^2\left[c_{\mathrm{n}}\sigma_n^2 + c_{\mathrm{t}}\boldsymbol{\tau}_n\cdot\boldsymbol{\tau}_n\right] - R\left(\alpha_n\right) \tag{12}$$

and in the incremental form

$$\mathrm{d}\Phi_{\mathrm{d}} = 3c_{\mathrm{n}}\alpha_n^2 S_n\left(\mathbf{T},\mathrm{d}\mathbf{T}\right) + D_n\left(\mathbf{T},\alpha_n\right)\mathrm{d}\alpha_n\,, \tag{13}$$

where $\mathbf{T} = (\sigma_n, \boldsymbol{\tau}_{\mathrm{n}})$, $S_n = \sigma_n \mathrm{d}\sigma_n + \dfrac{c_{\mathrm{t}}}{c_{\mathrm{n}}}\boldsymbol{\tau}_n\cdot\mathrm{d}\boldsymbol{\tau}_n$ and $D_n = 3\alpha_n\left(c_{\mathrm{n}}\sigma_n^2 + c_{\mathrm{t}}\boldsymbol{\tau}_n\cdot\boldsymbol{\tau}_n\right) - R'\left(\alpha_n\right)$,

We can thus write (when $\Phi_{\mathrm{d}} = 0$)

$$\mathrm{d}\Phi_{\mathrm{d}} \leq 0, \quad \mathrm{d}\alpha_n \geq 0, \quad \mathrm{d}\Phi_{\mathrm{d}}\mathrm{d}\alpha_n = 0\,. \tag{14}$$

The solution of crack growth eqns (13), (14) is shown in Table 1.

In order to analyse the slip on a rough inclined crack surface, let us introduce two coordinate systems. The system $0xyz$ referred to the nominal contact surface Γ_0 and the system $0\hat{x}\hat{y}\hat{z}$ referred to the actual surface $\hat{\Gamma}_0$ inclined at the angle φ to Γ_0 (see Figure 2). These two systems have the common axis $y = \hat{y}$, and the axis $\hat{x}$ is inclined at the dilatancy angle φ to the x-axis. It is assumed that slip direction coincides with the $\hat{x}$-axis and the shear strain vector coincides with the x-axis, thus: $\hat{\gamma}_{n2}^{\mathrm{d}} = \gamma_{n2}^{\mathrm{d}} = 0$, $\hat{\gamma}_{n1}^{\mathrm{d}} = \hat{\gamma}_n^{\mathrm{d}}$, $\gamma_{n1}^{\mathrm{d}} = \gamma_n^{\mathrm{d}}$. We have the following relations between strain components

$$\begin{Bmatrix} \hat{\gamma}_{n1}^{\mathrm{d}} \\ \hat{\gamma}_{n2}^{\mathrm{d}} \\ \hat{\varepsilon}_n^{\mathrm{d}} \end{Bmatrix} = \begin{bmatrix} \cos\varphi & 0 & \sin\varphi \\ 0 & 1 & 0 \\ -\sin\varphi & 0 & \cos\varphi \end{bmatrix} \begin{Bmatrix} \gamma_{n1}^{\mathrm{d}} \\ \gamma_{n2}^{\mathrm{d}} \\ \varepsilon_n^{\mathrm{d}} \end{Bmatrix}. \tag{15}$$

The identical relations occur between the contact tractions, the stress components and the strain increments. The vector $\hat{\mathbf{f}}_n$ is coaxial with $\mathrm{d}\hat{\boldsymbol{\gamma}}_n^{\mathrm{d}}$ and during contact slip we have

$$\hat{\varepsilon}_n^{\mathrm{d}} = 0, \qquad \varepsilon_n^{\mathrm{d}} = \left|\boldsymbol{\gamma}_n^{\mathrm{d}}\right| \tan\varphi\,. \tag{16}$$

Table 1: Solution of the incremental crack growth equations.

	$D_n < 0$	$D_n = 0$	$D_n > 0$
$S_n < 0$	$\mathrm{d}\alpha_n = 0$	$\mathrm{d}\alpha_n = 0$	$\mathrm{d}\alpha_n = 0$ or $\mathrm{d}\alpha_n = -3c_n\alpha_n^2 S_n D_n^{-1}$
$S_n = 0$	$\mathrm{d}\alpha_n = 0$	$\mathrm{d}\alpha_n \geq 0$	$\mathrm{d}\alpha_n = 0$
$S_n > 0$	$\mathrm{d}\alpha_n = -3c_n\alpha_n^2 S_n D_n^{-1}$	No solution	No solution

The limit friction condition is

$$\hat{\Phi}_{\mathrm{s}} = \left|\hat{\mathbf{f}}_n\right| + \hat{p}_n \tan\psi = \left|\hat{\boldsymbol{\tau}}_n - \frac{\hat{\boldsymbol{\gamma}}_n^{\mathrm{d}}}{\alpha_n^3 \hat{c}_{\mathrm{t}}}\right| + \left(\hat{\sigma}_n + \frac{\left|\hat{\boldsymbol{\gamma}}_n^{\mathrm{d}}\right|}{\alpha_n^3 \hat{c}_{\mathrm{n}}}\right)\tan\psi \le 0 \tag{17}$$

where $\dfrac{1}{\hat{c}_{\mathrm{t}}} = \dfrac{\cos^2\varphi}{c_{\mathrm{t}}} + \dfrac{\sin^2\varphi}{c_{\mathrm{n}}}, \qquad \dfrac{1}{\hat{c}_{\mathrm{n}}} = \sin\varphi\cos\varphi\left(\dfrac{1}{c_{\mathrm{t}}} - \dfrac{1}{c_{\mathrm{n}}}\right).$

The slip occurs when $\hat{\Phi}_{\mathrm{s}} = \mathrm{d}\hat{\Phi}_{\mathrm{s}} = 0$. We have in the plane $\hat{\Gamma}_0$

$$\mathrm{d}\hat{\varepsilon}_n^{\mathrm{d}} = 0, \qquad \mathrm{d}\hat{\boldsymbol{\gamma}}_n^{\mathrm{d}} = \hat{\mathbf{v}}_n \mathrm{d}\hat{\lambda}_n = \frac{\hat{\mathbf{f}}_n}{\left|\hat{\mathbf{f}}_n\right|}\mathrm{d}\hat{\lambda}_n, \qquad \mathrm{d}\hat{\lambda}_n \ge 0\,. \tag{18}$$

The increment of $\hat{\Phi}_{\mathrm{s}}$ equals

$$\mathrm{d}\hat{\Phi}_{\mathrm{s}} = \mathrm{d}\hat{t}_n - A_{11}^{(n)}\mathrm{d}\hat{\lambda} - A_{12}^{(n)}\mathrm{d}\alpha_n\,, \tag{19}$$

$$\mathrm{d}\hat{t}_n = \mu \mathrm{d}\hat{\sigma}_n + \hat{\mathbf{v}}_n \cdot \mathrm{d}\hat{\boldsymbol{\tau}}_n, \quad A_{11}^{(n)} = \frac{1}{\alpha_n^3 \hat{c}_{\mathrm{t}}} - \frac{\mu\hat{\boldsymbol{\gamma}}_n^{\mathrm{d}} \cdot \hat{\mathbf{v}}_n}{\alpha_n^3 \hat{c}_{\mathrm{n}}\left|\hat{\boldsymbol{\gamma}}_n^{\mathrm{d}}\right|}, \quad A_{12}^{(n)} = -\frac{3\hat{\boldsymbol{\gamma}}_n^{\mathrm{d}} \cdot \hat{\mathbf{v}}_n}{\alpha_n^4 \hat{c}_t} + \frac{3\left|\hat{\boldsymbol{\gamma}}_n^{\mathrm{d}}\right|}{\alpha_n^4 \hat{c}_n}. \tag{20}$$

The crack growth condition (19) is expressed in terms of $\hat{\boldsymbol{\gamma}}_n^{\mathrm{d}}$ as follows

$$\Phi_{\mathrm{d}} = \frac{3}{2}\frac{\hat{\boldsymbol{\gamma}}_n^{\mathrm{d}} \cdot \hat{\boldsymbol{\gamma}}_n^{\mathrm{d}}}{\alpha_n^4 \hat{c}_{\mathrm{t}}} - R(\alpha_n) \le 0 \tag{21}$$

and the increment equals

$$\mathrm{d}\Phi_{\mathrm{d}} = -A_{21}^{(n)}\mathrm{d}\hat{\lambda}_n - A_{22}^{(n)}\mathrm{d}\alpha_n\,, \tag{22}$$

$$A_{21}^{(n)} = -\frac{3}{\alpha_n^4 \hat{c}_{\mathrm{t}}}\hat{\mathbf{v}}_n \cdot \hat{\boldsymbol{\gamma}}_n^{\mathrm{d}}, \quad A_{22}^{(n)} = \frac{6}{\alpha_n^5 \hat{c}_{\mathrm{t}}}\hat{\boldsymbol{\gamma}}_n^{\mathrm{d}} \cdot \hat{\boldsymbol{\gamma}}_n^{\mathrm{d}} + R'(\alpha_n) > 0. \tag{23}$$

The following cases can now be considered:

i) $\Phi_{\mathrm{d}} < 0, \quad \hat{\Phi}_{\mathrm{s}} < 0$; there is no slip and crack growth ($\mathrm{d}\alpha_n = \mathrm{d}\hat{\lambda}_n = 0$),

ii) $\Phi_{\mathrm{d}} = 0, \quad \hat{\Phi}_{\mathrm{s}} < 0$; there is no slip, so there is no crack growth ($\mathrm{d}\alpha_n = \mathrm{d}\hat{\lambda}_n = 0$),

iii) $\Phi_{\mathrm{d}} < 0, \quad \hat{\Phi}_{\mathrm{s}} = 0$; the slip may occur ($\mathrm{d}\hat{\lambda}_n \ge 0$), but there is no crack growth ($\mathrm{d}\alpha_n = 0$),

iv) $\Phi_{\mathrm{d}} = 0, \quad \hat{\Phi}_{\mathrm{s}} = 0$; the slip and crack growth may occur simultaneously ($\mathrm{d}\hat{\lambda}_n \ge 0$, $\mathrm{d}\alpha_n \ge 0$).

The increments $\mathrm{d}\hat{\lambda}_n$, $\mathrm{d}\alpha_n$ satisfy the following complementary conditions

$$\mathrm{d}\hat{\Phi}_{\mathrm{s}}\mathrm{d}\hat{\lambda}_n = 0, \quad \mathrm{d}\Phi_{\mathrm{d}}\mathrm{d}\alpha_n = 0, \quad \mathrm{d}\hat{\Phi}_{\mathrm{s}} \le 0, \quad \mathrm{d}\Phi_{\mathrm{d}} \le 0, \quad \mathrm{d}\hat{\lambda}_n \ge 0, \quad \mathrm{d}\alpha_n \ge 0\,, \tag{24}$$

and one of the following solutions is obtained (see Table 2):

$$\mathrm{d}\hat{\lambda}_n = 0, \qquad \mathrm{d}\alpha_n = 0\,, \tag{25a}$$

$$\mathrm{d}\hat{\lambda}_n = \frac{\mathrm{d}\hat{t}_n}{A_{11}^{(n)}}, \qquad \mathrm{d}\alpha_n = 0\,, \tag{25b}$$

Table 2: Solution types of the set (24).

$\det\mathbf{A}_n > 0$			
	$\hat{t}_n < 0$	$\hat{t}_n = 0$	$\hat{t}_n > 0$
$\hat{\mathbf{v}}_n \cdot \hat{\boldsymbol{\gamma}}_n^{\mathrm{d}} < 0$, thus $A_{21}^{(n)} > 0$	(25a)	(25a)	(25b)
$\hat{\mathbf{v}}_n \cdot \hat{\boldsymbol{\gamma}}_n^{\mathrm{d}} = 0$, thus $A_{21}^{(n)} = 0$	(25a)	(25a)	(25b)
$\hat{\mathbf{v}}_n \cdot \hat{\boldsymbol{\gamma}}_n^{\mathrm{d}} > 0$, thus $A_{21}^{(n)} < 0$	(25a)	(25a)	(25c)
$\det\mathbf{A}_n = 0$			
$\hat{\mathbf{v}}_n \cdot \hat{\boldsymbol{\gamma}}_n^{\mathrm{d}} < 0$, thus $A_{21}^{(n)} > 0$	(25a)	(25a)	(25b)
$\hat{\mathbf{v}}_n \cdot \hat{\boldsymbol{\gamma}}_n^{\mathrm{d}} = 0$, thus $A_{21}^{(n)} = 0$	(25a)	(25a),(25d)	(25b)
$\hat{\mathbf{v}}_n \cdot \hat{\boldsymbol{\gamma}}_n^{\mathrm{d}} > 0$, thus $A_{21}^{(n)} < 0$	(25a)	(25a),(25d)	No solution
$\det\mathbf{A}_n < 0$			
$\hat{\mathbf{v}}_n \cdot \hat{\boldsymbol{\gamma}}_n^{\mathrm{d}} < 0$, thus $A_{21}^{(n)} > 0$	(25a)	(25a)	(25b)
$\hat{\mathbf{v}}_n \cdot \hat{\boldsymbol{\gamma}}_n^{\mathrm{d}} = 0$, thus $A_{21}^{(n)} = 0$	(25a)	(25a)	(25b)
$\hat{\mathbf{v}}_n \cdot \hat{\boldsymbol{\gamma}}_n^{\mathrm{d}} > 0$, thus $A_{21}^{(n)} < 0$	(25a),(25c)	(25a)	No solution

$$\mathrm{d}\hat{\lambda}_n = \frac{A_{22}^{(n)}\mathrm{d}\hat{t}_n}{\det\mathbf{A}_n}, \qquad \mathrm{d}\alpha_n = -\frac{A_{21}^{(n)}\mathrm{d}\hat{t}_n}{\det\mathbf{A}_n}, \tag{25c}$$

$$\mathrm{d}\alpha_n = -\frac{A_{21}^{(n)}}{A_{22}^{(n)}}\mathrm{d}\hat{\lambda}_n, \qquad \hat{\lambda}_n \geq 0. \tag{25d}$$

3. MODELLING STRESS-STRAIN RESPONSE

Following Gambarotta and Logomarsino [2], we assume

$$R(\alpha_n) = \kappa(\alpha_n - 1)^{1/m}, \tag{26}$$

where κ and m are the material parameters. For the case of tension normal to the crack plane we have

$$R(\alpha_{\mathrm{c}}) = \frac{3}{2}\alpha_{\mathrm{c}}^2 c_{\mathrm{n}}\sigma_{\mathrm{c}}^2, \quad m = \frac{\alpha_{\mathrm{c}}}{2(\alpha_{\mathrm{c}} - 1)}, \quad \kappa = \frac{3}{2}c_{\mathrm{n}}\sigma_{\mathrm{c}}^2\tilde{\kappa}^2, \quad \tilde{\kappa} = \alpha_{\mathrm{c}}(\alpha_{\mathrm{c}} - 1)^{1/\alpha_{\mathrm{c}} - 1}. \tag{27}$$

Thus, the parameters κ and m can be specified once the critical crack size α_{c} and the critical stress σ_{c} have been determined experimentally.

Figure 3ab presents the stress-strain curves for an element with oriented set of cracks. Figure 4a present the dependence of crack size on its orientation. It was shown already that the critical orientation angle $\delta_{\mathrm{c}} = \pi/4 + (\varphi + \psi)/2$ corresponds to the largest microcrack growth and the orientation of the failure plane is specified by δ_{c}. Figure 4b presents the stress-strain diagrams for elements with uniformly distributed microcracks in uniaxial compression generated by the model equations.

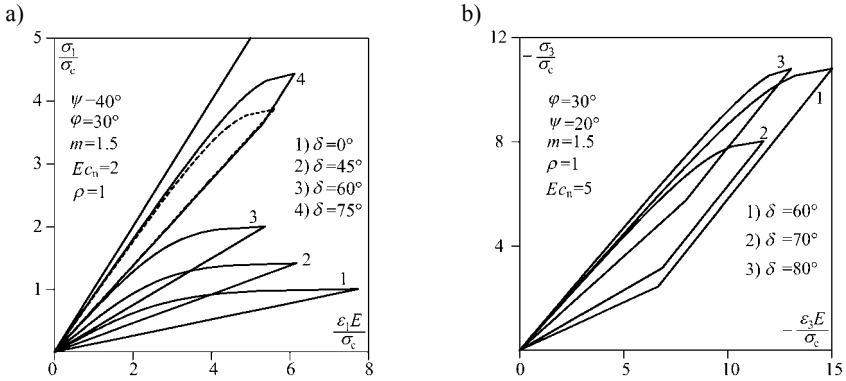

Figure 3: The stress-strain curves in uniaxial tension (a) and compression (b) for an element with oriented cracks.

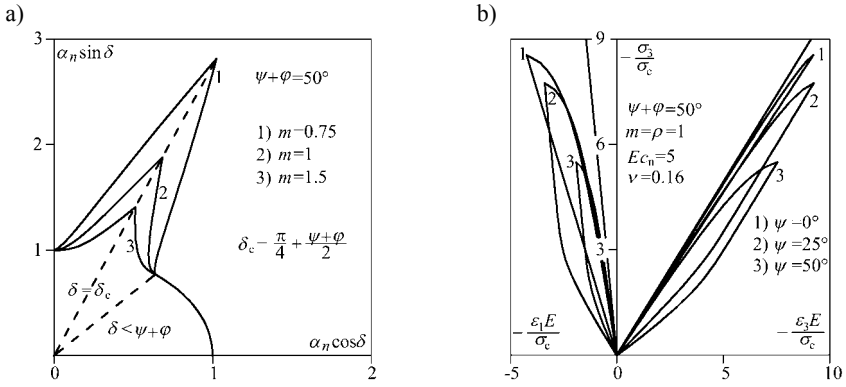

Figure 4: a) Crack size variation, b) loading-unloading stress-strain diagrams for uniaxial compression of uniformly cracked elements.

4. CONCLUDING REMARKS

The present analysis of microcracked materials extends previous studies by Andrieux et al. [1] and Gambarotta and Logomarsino [2] by accounting for dilatancy effect at crack interfaces. Both unilateral contact condition, friction slip and crack growth are included in the analysis. The isotropic and anisotropic microcrack distribution is considered. The crack branching effects leading to wing cracks are neglected by assuming crack growth in the same physical plane.

REFERENCES

[1] Andrieux, S., Bamberger, Y. and Marigo J.J., Un modéle de materiau microfissuré pour les bétons et les roches. *J. Méc. Theor. Appl.* **5,** 471-513,1986.

[2] Gambarotta, L. and Lagomarsino, S., A microcrack damage model for brittle materials. *International Journal of Solids and Structures* **30**, 177-198, 1993.

[3] Mróz, Z. and Seweryn, A., Non-local failure and damage evolution rule: Application to a dilatant crack model. *J. de Physique IV France*, **8**, 257-268, 1998.

Acknowledgement. The investigation described in this paper is a part of the research project No. 8 T07A 049 21 sponsored by the Polish State Committee for Scientific Research.